Communications Earth & Environment

Supplementary Information

Conjugate faulting and structural complexity on the young fault system associated with the 2000 Tottori earthquake

Aitaro Kato[1]*, Shin'ichi Sakai[1], Satoshi Matsumoto[2], Yoshihisa Iio[3]

1: Earthquake Research Institute, University of Tokyo,
1-1-1 Yayoi, Bunkyo-ku, Tokyo 113-0032, Japan.

2: Institute of Seismology and Volcanology, Kyushu University,
744 Moto-oka, Nishi-ku, Fukuoka 819-0395, Japan.

3: Disaster Prevention Research Institute, Kyoto University,
Gokasho, Uji, Kyoto 611-0011, Japan.

*Corresponding author: Aitaro Kato (akato@eri.u-tokyo.ac.jp)

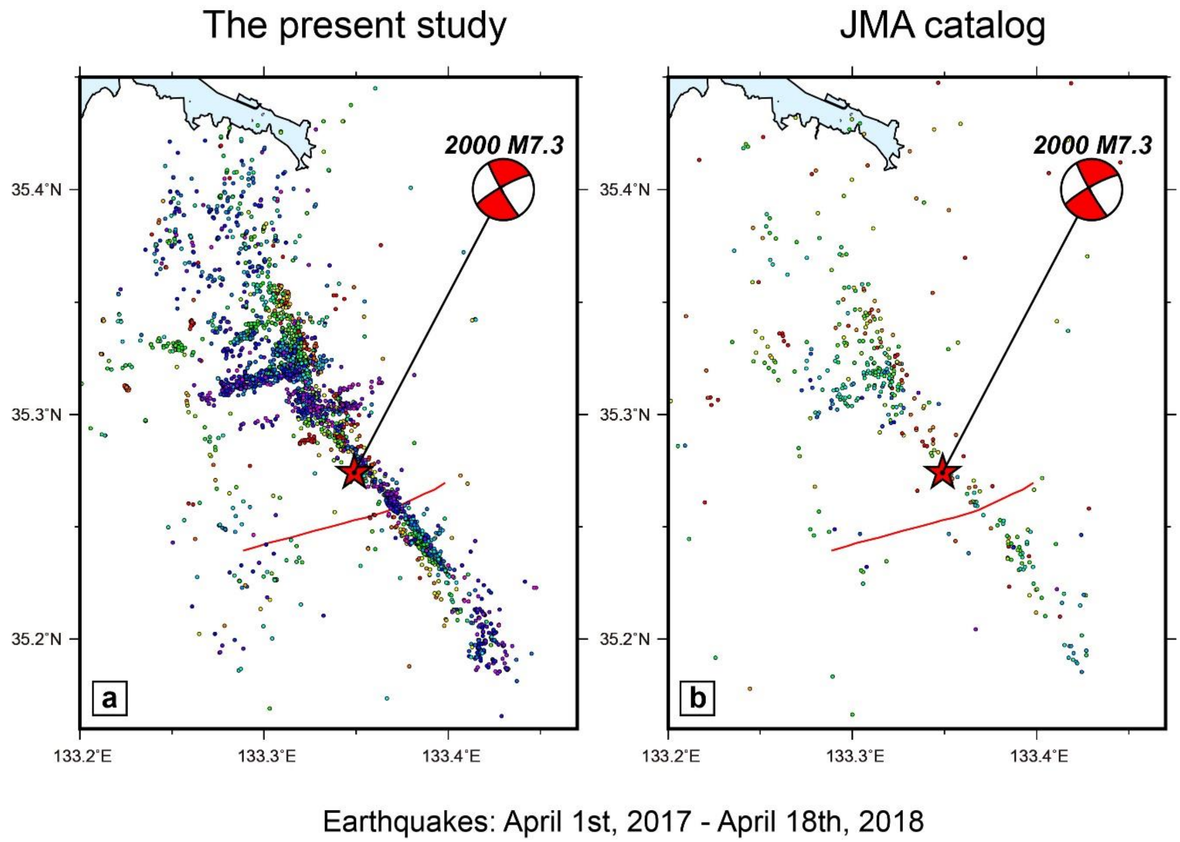

Supplementary Figure S1. Comparison of hypocenter distributions between the present study and the JMA catalog (from 1st April 2017 to 18th April 2018). a The present study. **b** The JMA catalog. Hypocenters are shown as circles that are scaled to earthquake magnitude and colored to hypocentral depth. Red star denotes an epicenter of the 2000 Tottori earthquake determined by JMA with CMT solution determined by NIED.

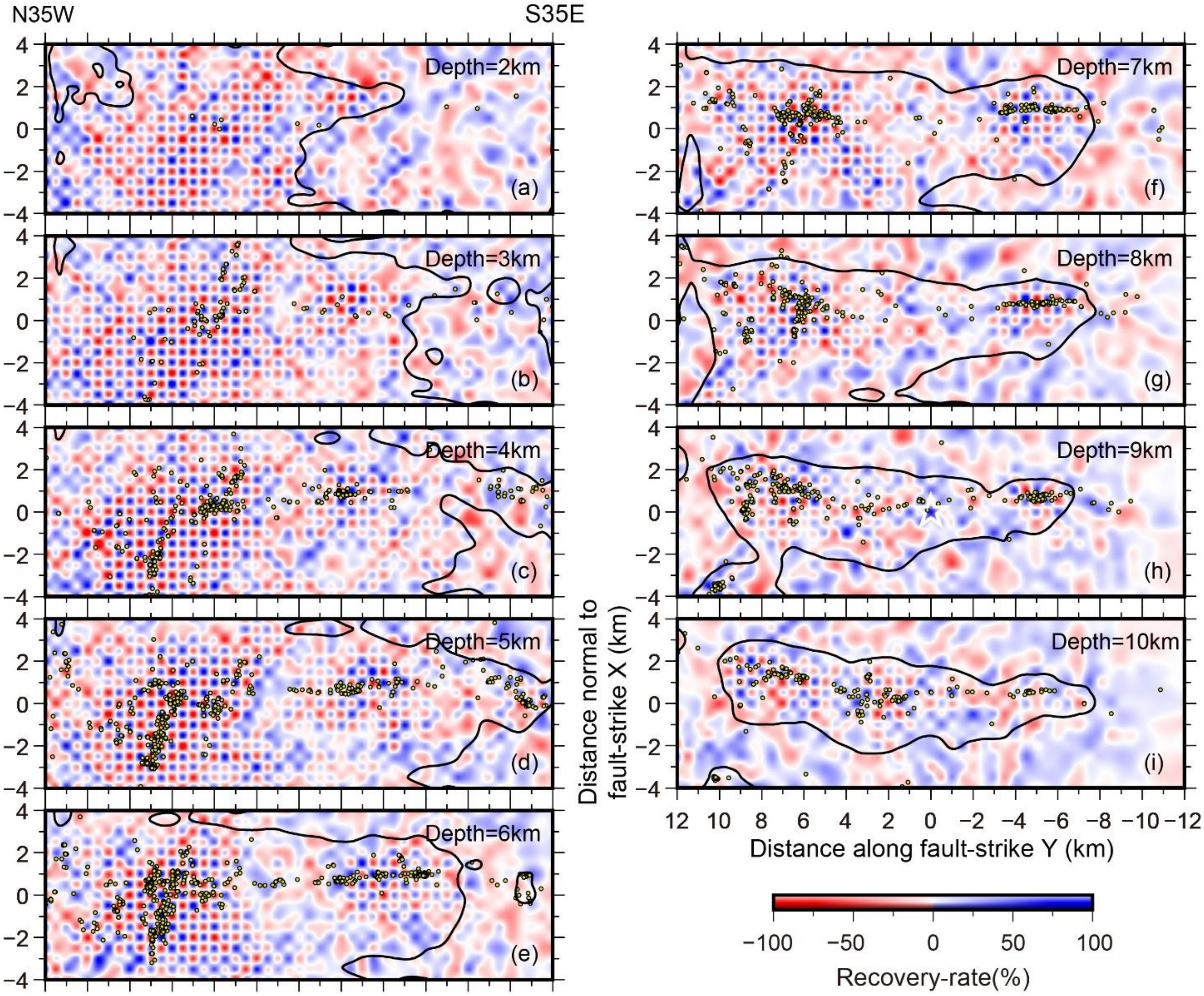

Supplementary Figure S2. Results of the checkerboard resolution test for the model shown in Fig. 3. The spatial smoothing weight is set to be 10. Solid line encloses the area in which the derivative weight sum (DWS)[1] values are sufficiently large.

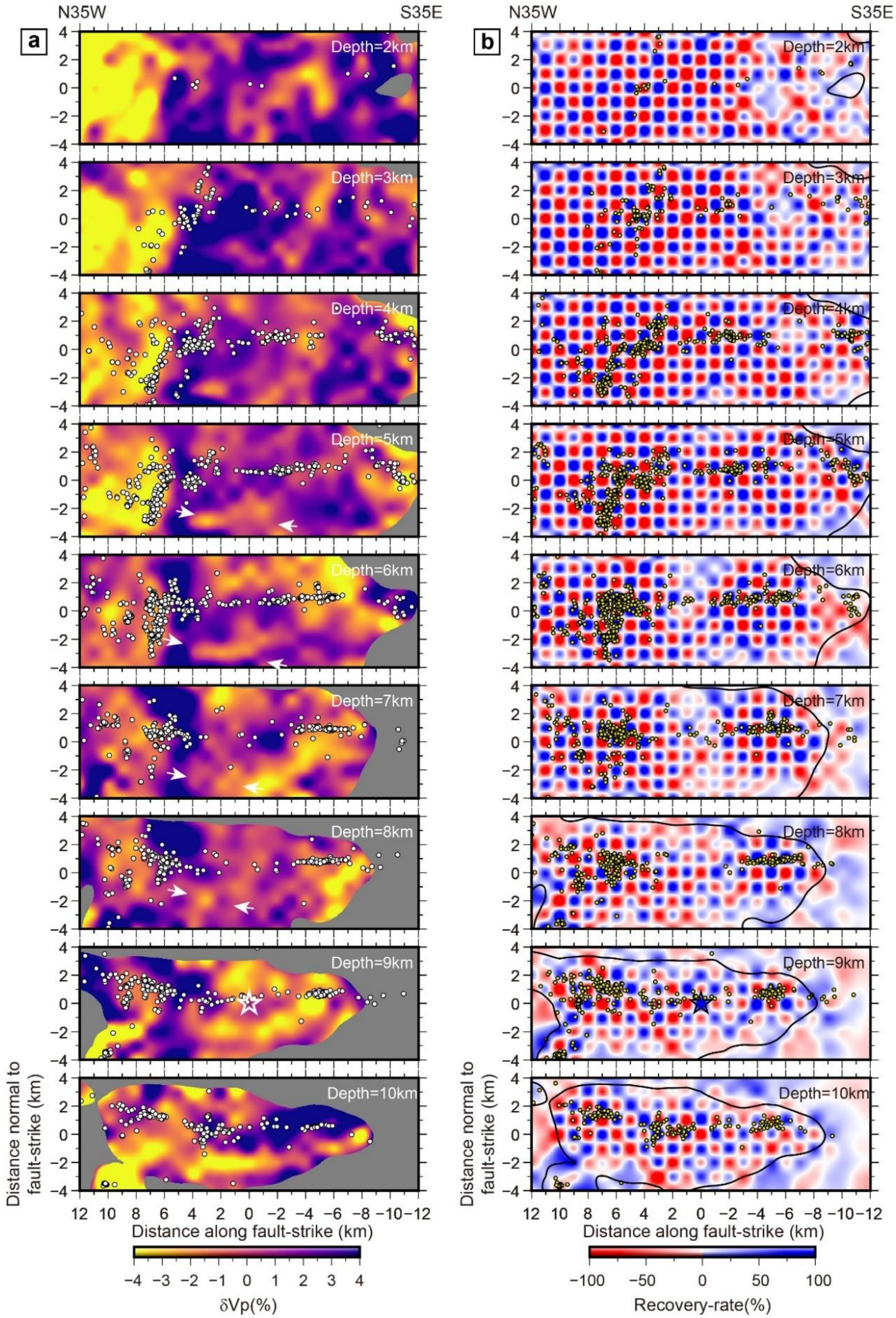

Supplementary Figure S3. **P-wave velocity model and result of checkerboard resolution test. a** P-wave velocity model rotated along the major aftershock alignment at each depth with a horizontal grid spacing of 1 km for the spatial smoothing weight of 10. White circles denote the relocated events within 0.5 km of each depth slice. White star denotes the epicenter of the 2000 Tottori earthquake determined by JMA. White arrows indicate a thin, low-velocity band that lies subparallel to the alignment of the main aftershocks. **b** Results of the checkerboard resolution test. Solid line encloses the area where the derivative weight sum (DWS)[1] values are sufficiently large.

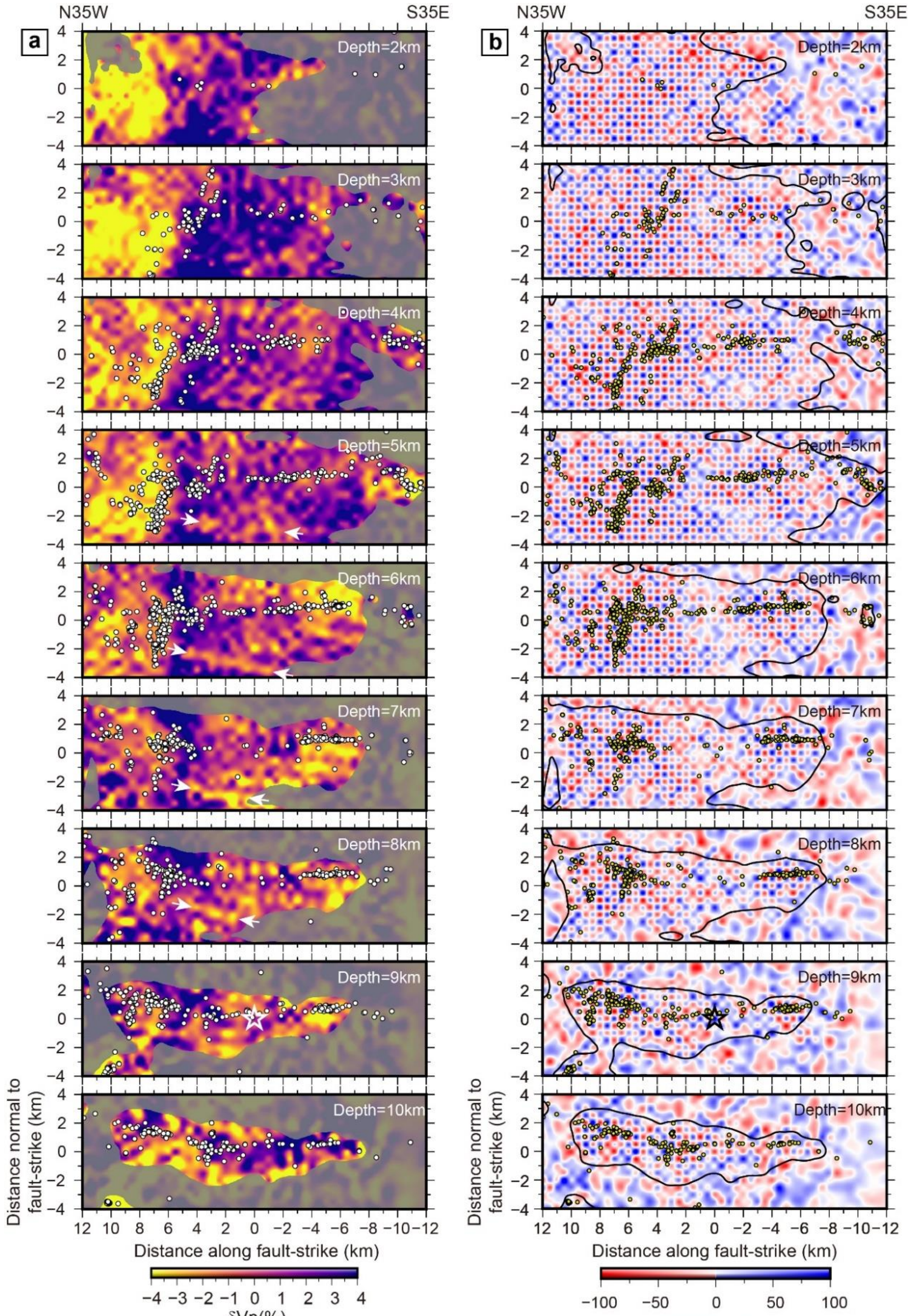

Supplementary Figure S4. P-wave velocity model and result of checkerboard resolution test. a P-wave velocity perturbation rotated along the major aftershock alignment at each depth with a horizontal grid spacing of 0.5 km for the spatial smoothing weight of 5. White circles denote the relocated events within 0.5 km of each depth slice. White star denotes the epicenter of the 2000 Tottori earthquake determined by JMA. White arrows indicate a thin, low-velocity band that lies subparallel to the alignment of the main aftershocks. **b** Results of the checkerboard resolution test. Solid line encloses the area in which the derivative weight sum (DWS)[1] values are sufficiently large.

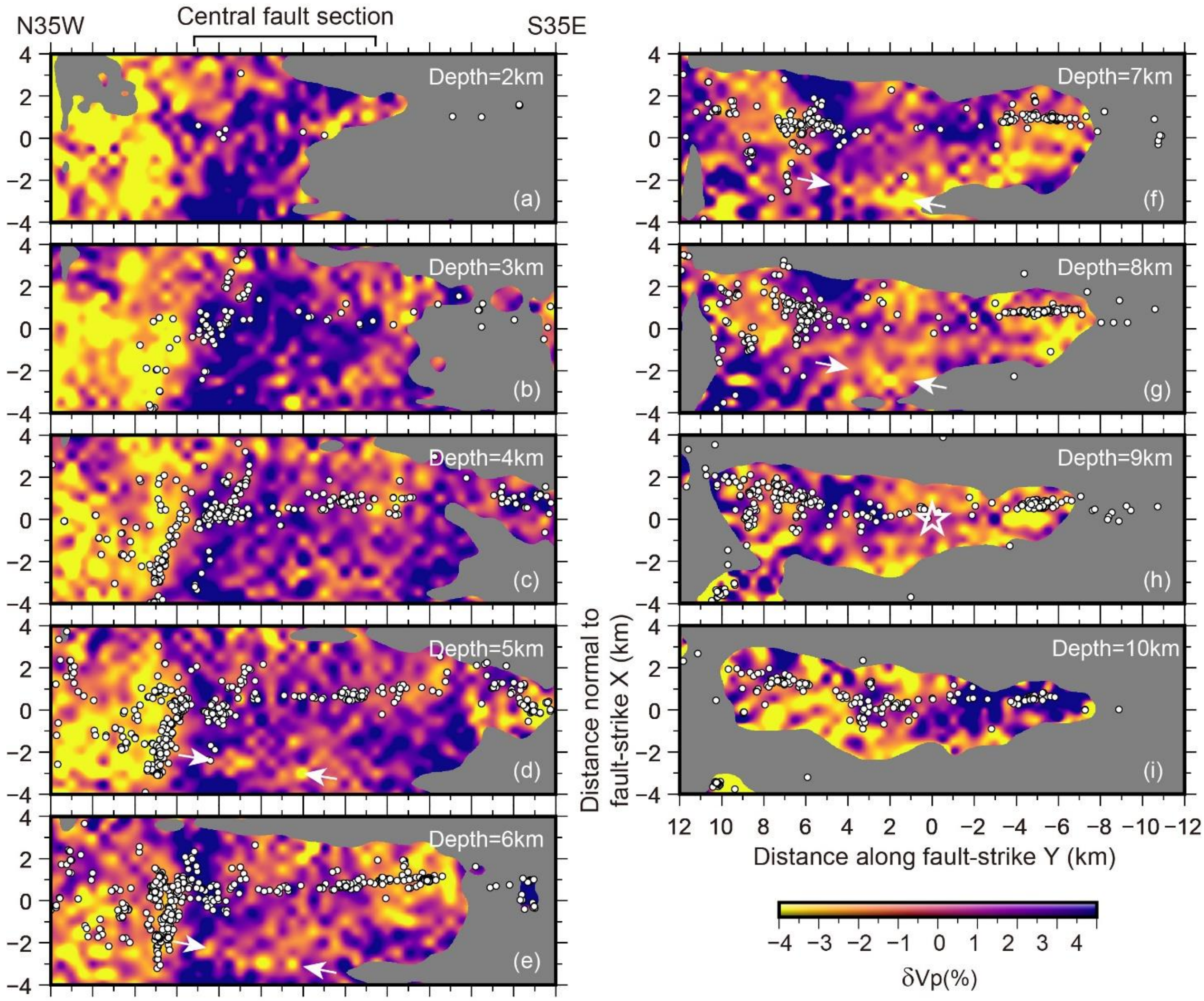

Supplementary Figure S5. P-wave velocity model at each depth. P-wave velocity perturbation rotated along the major aftershock alignment at each depth with a horizontal grid spacing of 0.5 km for the spatial smoothing weight of 1. White circles denote the relocated events within 0.5 km of each depth slice. White star denotes the epicenter of the 2000 Tottori earthquake determined by JMA.

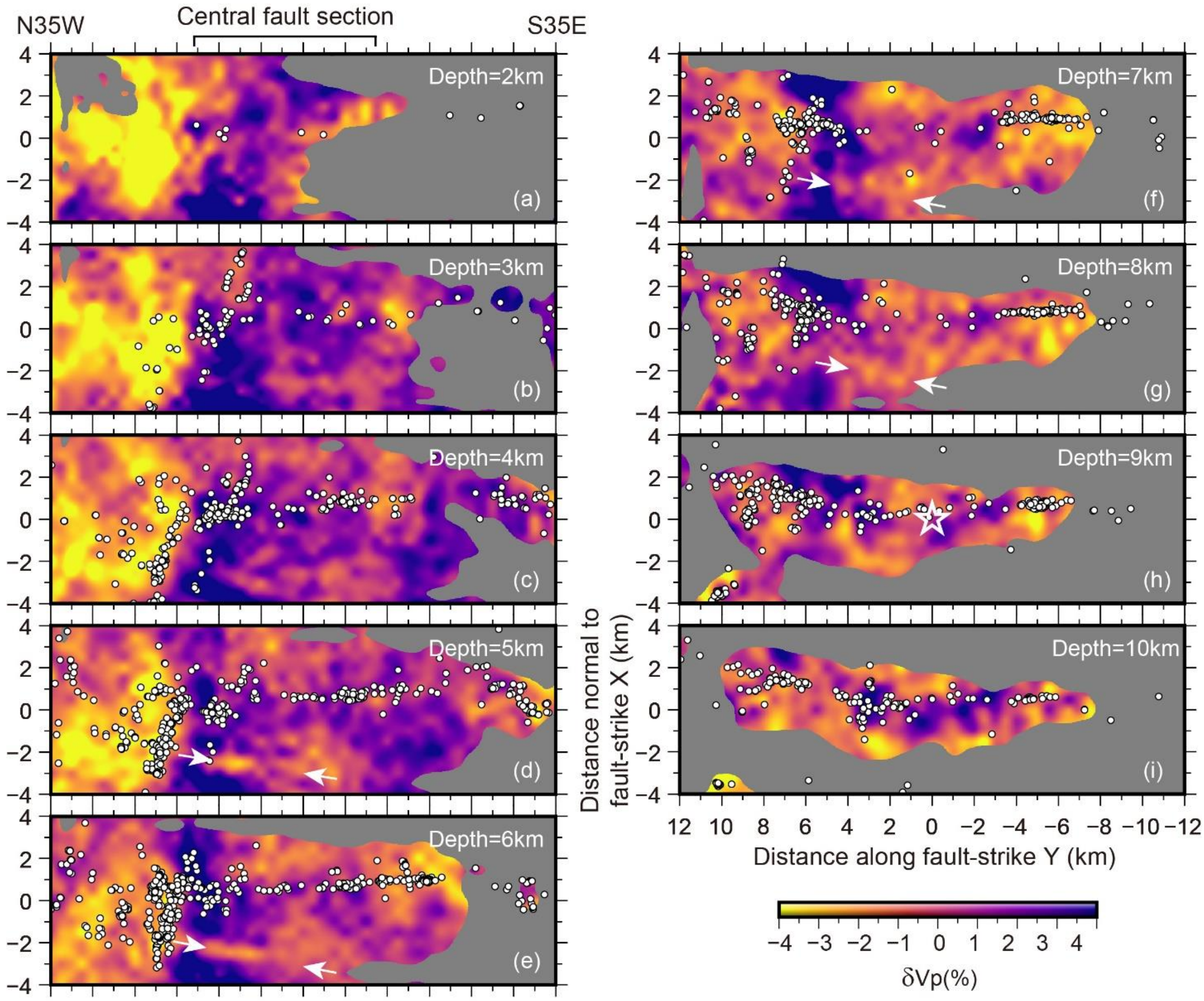

Supplementary Figure S6. P-wave velocity model at each depth. P-wave velocity perturbation rotated along the major aftershock alignment at each depth with a horizontal grid spacing of 0.5 km for the spatial smoothing weight of 20. White circles denote the relocated events within 0.5 km of each depth slice. White star denotes the epicenter of the 2000 Tottori earthquake determined by JMA.

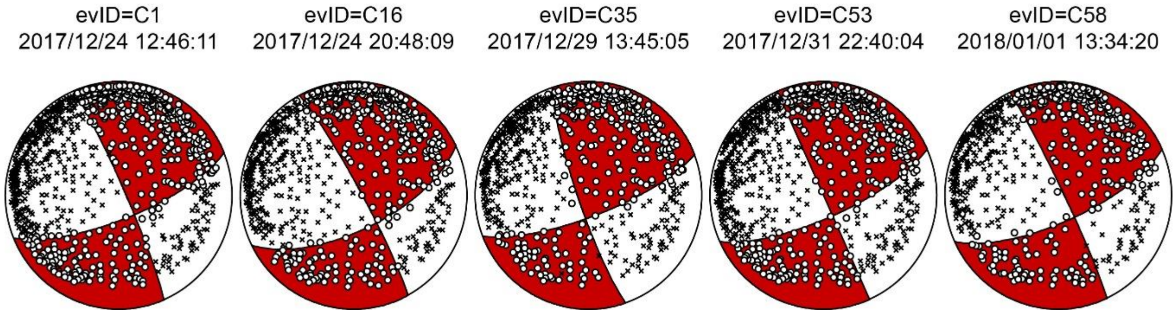

Supplementary Figure S7. Focal mechanism solutions determined by P-wave polarity data. For events with M_L greater than 1.3 during a sequence following the M_L2.2 event (Fig. 4). Circle and cross denote up and down of P-wave first motion polarities, respectively. The top number above each mechanism is the identification number and origin time of the event.

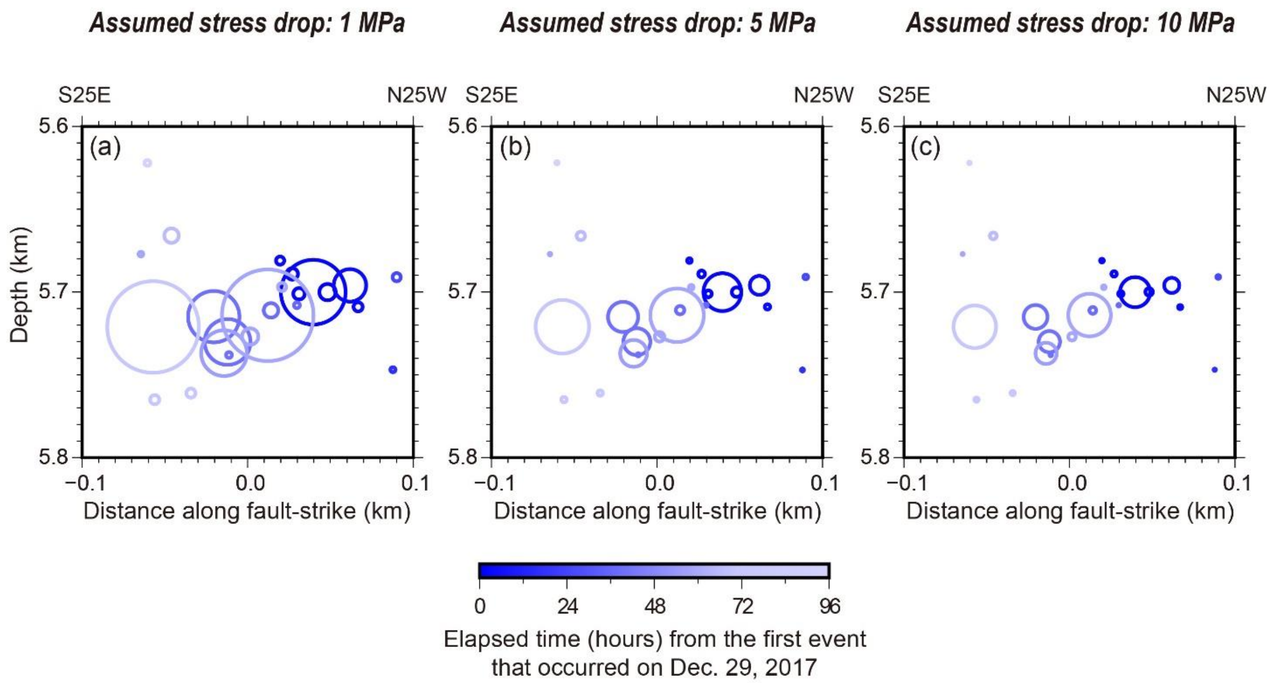

Supplementary Figure S8. Along strike sections of the ruptured areas during the earthquake migration in the tiny seismic cluster (Figs. 4d & 4e). For three cases assuming different stress drops; **a** 1 MPa, **b** 5 MPa, **c** 10 MPa. We calculated the fault radius of each event assuming a circular fault model and a relation between the magnitude and the seismic moment[2]. Edge of each rupture area is colored to a time elapsed from the first event showing the migration on 29 December 2017.

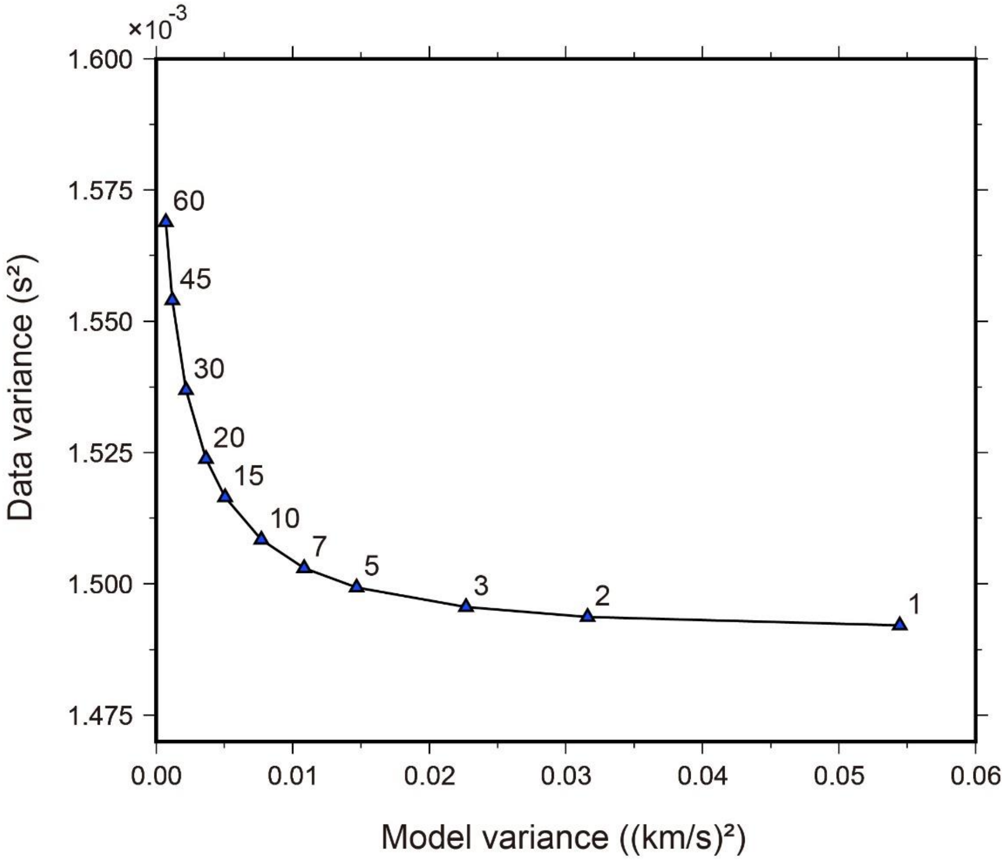

Supplementary Figure S9. Trade-off curve between solution variance and data variance for selecting optimal spatial smoothing weights. The spatial smoothing weights are included in the figure. We chose the velocity model with a smoothing weight of 10 for our preferred final model.

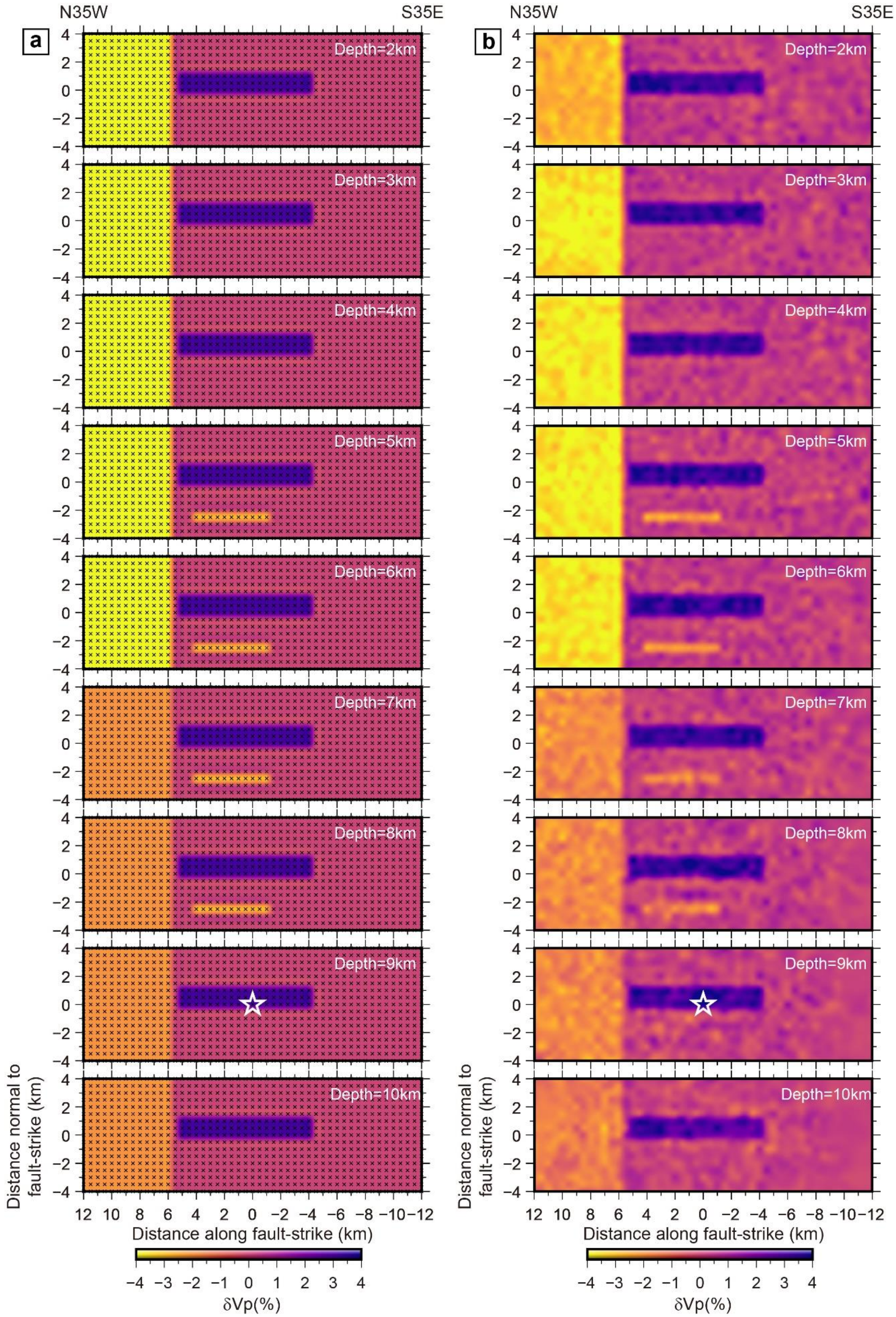

Supplementary Figure S10. Results of a sensitivity test (spike test). a Input P-wave anomalies. Crosses denote the grid used in the tomography analysis. **b** Test results.

Depth (km)	Vp (km/s)
0.00	4.80
1.00	5.10
2.00	5.35
3.00	5.55
4.00	5.70
5.00	5.82
6.00	5.85
7.00	5.90
8.00	5.93
9.00	5.97
10.00	6.02
12.00	6.10
15.00	6.22
20.00	6.45

Supplementary Table S1. The initial one-dimensional velocity structure (JMA) employed in the present study. P-wave velocity at each depth is listed up.

Supplementary References

1. Thurber, Clifford, Eberhart-phillips, D. Local earthquake tomography with exible gridding. *Comput. Geosci.* **25**, 809–818 (1999).

2. Hanks, T. C. & Kanamori, H. A moment magnitude scale. *J. Geophys. Res.* **84**, 2348–2350 (1979).